

# SIMULATIONS AND DESIGN OF THZ WIGGLER FOR 15-40 MEV FEL

E.M. Syresin, N.A. Morozov, R.S. Makarov, S.A. Kostromin, D.S. Petrov  
 Joint Institute for Nuclear Research, Dubna, Russia

## Abstract

The electromagnetic wiggler is applied for narrow-band THz radiation in the 30 μm to 9.35 mm wavelength range. This is a planar electromagnetic device with 6 regular periods, each 30 cm long. The end termination pattern structure is +1/4,-3/4,+1,...,-1,+3/4,-1/4. This structure is more appreciable for compensation of the first and second fields, especially, to provide the small value of second integral of 500 G×cm<sup>2</sup>. The peak magnetic field is up to 0.356 T, it is defined by large wiggler gap of 102 mm and a capacity of water cooling system of 70 kW. The parameter is varied in the range K=0.5- 7.12 corresponding to a field range B=0.025- 0.356 T peak field on axis. The wiggler is used in 15-40 MeV. The bunch compression scheme allows the whole wavelength range to be covered by super-radiant emission with a sufficient form factor. The wavelength range corresponds to 217 μm-9.35 mm at electron energy of 15 MeV, it is equal to 54 μm-2.3 mm at electron energy of 30 MeV and it is 30 μm-1.33 mm at electron energy of 40 MeV. The 3D Opera simulations of THz wiggler is under discussion.

## INTRODUCTION

The design of THz wiggler and technical solution at its construction are based on FIR FLASH undulator constructed in JINR [1-5].

Table 1: Summary of wiggler technical data.

Parameter of THz wiggler	value
period length, mm	300
number of full periods	7
number of poles including end-pieces	14+4
maximum wiggler parameter $K_{RMS}$	7.12
peak field on axis, T	0.356
height of magnetic axis above floor level, m	1.4
minimum clear gap, mm	102
position accuracy of magnetic axis, mm	0.5
angular precision of magnetic axis, mrad	0.5
field flatness at ±20 mm off-axis (horizontally), %	-0.1... +0.5
first field integral I1, G×cm	50
second field integral I2, G×cm <sup>2</sup>	500
stability and reproducibility of magnetic axis, mm/μrad	±0.1/ ±50

The second peculiarity of wiggler is related to the trim coils. The four trim coils with individual power supply should be installed in wiggler. These trim coils permit to compensate on the full wiggler length the first and second integrals. However it does not permit to compensate integral on period length. The first integral on period length should be smaller than 50 G×cm and also very low second integral 500 G×cm<sup>2</sup>. To provide both these requirements it is propose to install in each regular coil an additional correction coil. The individual correction coils should compensate imperfection of wiggler mechanical construction and errors in coil position. In the parallel to each individual correction coil a variable resistance divider will be installed. As a result through each individual correction coil will pass the individual optimal correction current; however for all 7 pairs of correction coils will use only 1 power supply system.

The 3D wiggler simulations at its full scale were performed by TOSCA code (Fig.1). The maximal available magnetic field corresponds to 0.356 T at number of Ampere×turns of  $I_w=1.85 \cdot 10^3$ . An increase of the number of Ampere turns up  $I_w=2.1 \cdot 10^3$  permits to linearly increase the magnetic field up the value of 0.375 T (Fig.1, Table 1).

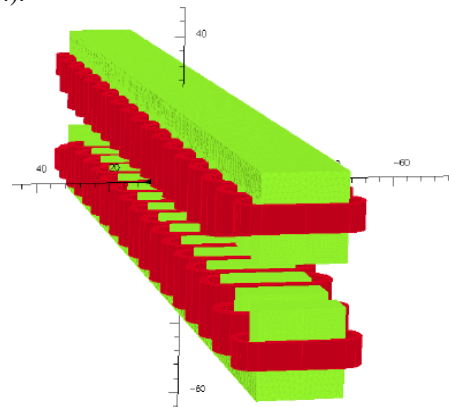


Figure 1: TOSCA 3D simulation of THz wiggler.

The 3 layer coil at the magnetic field of 0.356 T corresponds to following water cooling system parameters: dissipated power of 70 kW, water cooling flow of 2.6 l/min through one coil (about 94 l/min for 36 coils) and temperature rise of 12<sup>o</sup>. So the maximum available magnetic field is defined by water cooling system. The increase of the magnetic field up to 0.375 T is required an increase of dissipated power up 96 kW and temperature up 16<sup>o</sup>.

The diffraction spot size of radiation defines the diameter of vacuum chamber and wiggler gap. The diffraction angle and spot radius of wiggler radiation are equal to

$\theta_d \equiv (\lambda/\pi L)^{0.5}$ ,  $r_d \equiv (\lambda L/\pi)^{0.5}$ , where  $L = 2.1$  m is the wiggler length,  $\lambda$  is the wave length. The diffraction parameters are equal to 3.5 mrad/7 mm at  $\lambda = 80 \mu\text{m}$ , 2 mrad/2.5 cm at wavelength of 1 mm and 20 mrad/4 cm at wavelength of 2.3 mm.

## MAIN COILS

The parameters of main coils are given in Table 2 for 3 winding layers. The coil design with 3 winding layers provides parameters of the water cooling system of 70 kW.

Table 1. Parameters of main coils.

Number of layers	3
$B_0$ (G)	3560
Conductor cross section, mm	8.5*8.5/D5.3
Coil cross-section with isolation (mm)	30*130
Number of turns	42 (3*14)
Number of $A \times$ turns	18500
Current, A	440
Total voltage (V)	160
Current density, A/mm <sup>2</sup>	8.9
1 coil power (kW)	2.2
Total power (kW)	70
Water cooling l/min (1 coil)	2.6
Temperature rise, C	12
Weight (kg) 1 coil	13.7
Total copper weight (kg)	440

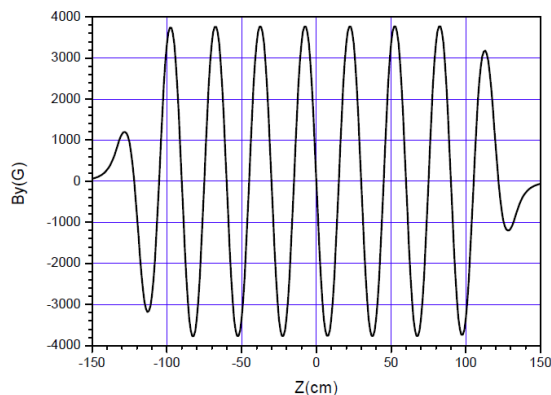


Figure 2: Wiggler magnetic field

For electron beam transport through a wiggler especially at low beam energies the transverse field profile is of great importance. Considering the wiggler amplitude at low beam energies and high wiggler parameters the good-

field region must be defined to extend  $\pm 20$  mm off-axis horizontally. The wiggler design discussed below with rectangular poles of 200 mm width shows a field roll-off by -0.2% at 20 mm off-axis. This can not be handled by the beam delivery for beam energies below 25 MeV. This consideration puts a limit of -0.1% at 20 mm to the off-axis field roll-off. In accordance with 3 D TOSCA simulation the transverse magnetic field variation is smaller than -0.1% at aperture of 20 mm.

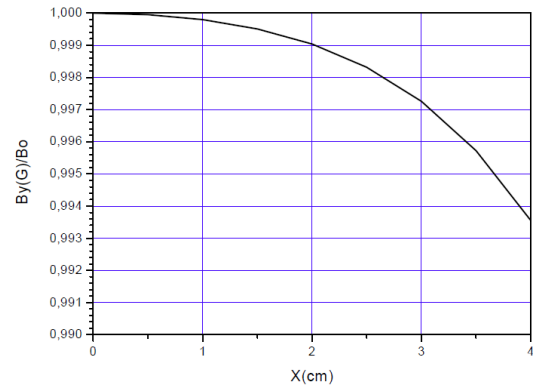


Figure 3: Dependence of normalized wiggler magnetic field at  $I_w = 21.5$  kA  $\times$  turns on transverse coordinate.

## TRIM AND CORRECTION COILS

Four correction coils should be able to drive 2% of the magnetic flux of a single pole from a 10 A supply. The trim coils 1 and 4 are installed on the first 3 poles and on the last 3 poles correspondingly. The trim coils 2 and 3 are placed on 4-9 poles and on 10-15 poles. The parameters of trim coils are given in Table 2 and Fig.4 and Fig.5. The currents in each corrector trim coils were optimizing to reduce the first and second integrals.

Table 2. Parameters of trim coils.

Parameter	Coil 1-4/coil 2-3
Corrected field (G)	15/10
$A \times$ turns (one coil)	105
Number of turns (one coil)	15
Current (A)	7
Conductor D(mm)/ $S_{con}$ (mm <sup>2</sup> )	2/3.1
$J$ (A/mm <sup>2</sup> )	2.2
Voltage (two coils) (V)	2/3
Power (two coils) (W)	14/21
Coil cross-section (mm)	2 $\times$ 30

Individual correction coils (14 pairs) on regular poles are placed overhand main regular coils and higher the corrected trim coils. The inputs from individual correction coils in to the first integrals along longitudinal axis are

given in Fig.6. The parameters of individual correction coil are presented in the Table 3.

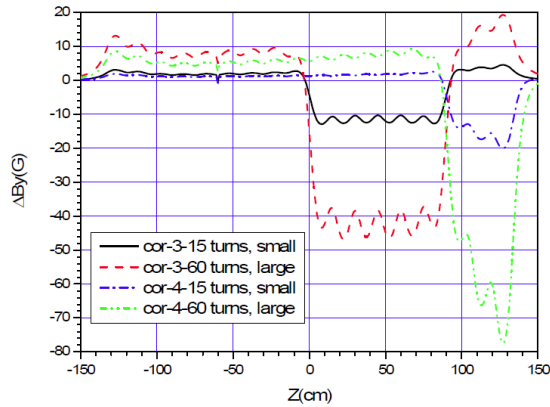


Figure 4: Magnetic field of correction trims coils.

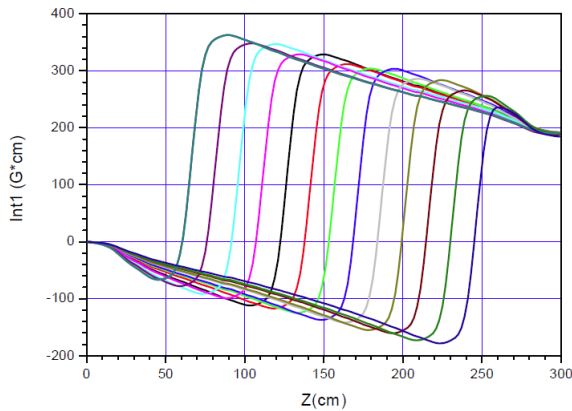


Figure 5: Second integral produced by trims coils.

Table 3. Parameters of the regular correction coils and the edge coils.

Parameter	Regular coil	Pole 1	Pole 2
Corrected field (G)	28	700	480
A×turns (one coil)	308	3696	3696
Number of turns (1 coil)	110	528	384
Current (A)	2.8	7	7
Conductor D(mm)	1.5	2	2
S <sub>conductor</sub> (mm <sup>2</sup> )	1.75	3.14	3.14
J (A/mm <sup>2</sup> )	1.6	2.2	2.2
Voltage (two coils) (V)	3.75	32	21
Power (two coils) (W)	10.5	220	150
Coil cross-section (mm)	3×85	11×96	13×116

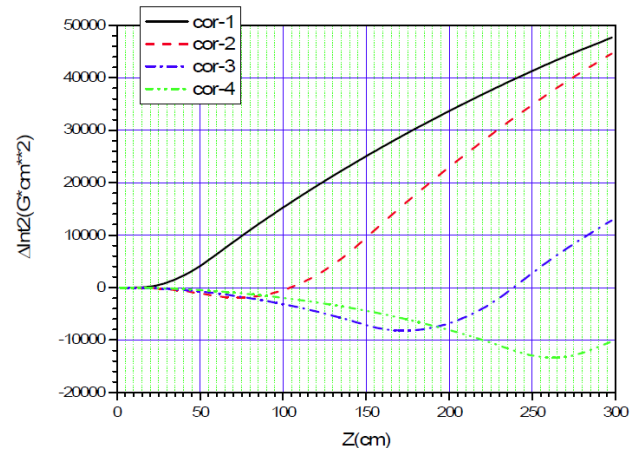


Figure 6: First integral of individual correction coils ( $I_w=308 \text{ A}\times\text{turnes}$ ).

Correction coils of first-last poles and second – seventeen poles are placed overhand main coils and higher to the corrected trim coils. The inputs from these correction coils in to the second integrals along longitudinal axis are given in Fig.7.

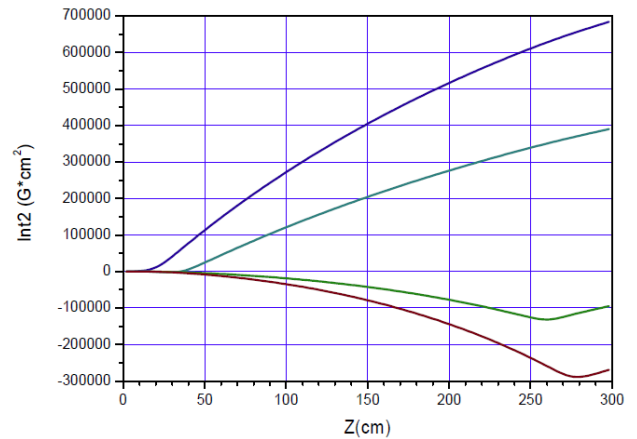


Figure 7: Second integral produced by correction trims coils.

### REFERENCES

- [1] O.Grimm et al, NIM A 615, is.1, (2010) 105.
- [2] M.Gensh et al, Infrared physics and technology, v.51, Iss.5, (2008) 423.
- [3] O.Brovko, et al, Particle and Nuclei Letters, v.7 № 1, (2010) 78.
- [4] O.Brovko et al, Applied physics, №3, (2010), 46.
- [5] R. Makarov et al, Particle and Nuclei Letters,, v.7 №7, (2010) 737.